

3

Photonic Systems for Crystalline Silicon and Thin-Film Photovoltaic Manufacturing

Peter Bermel, Gary J. Cheng, and Xufeng Wang

CONTENTS

Introduction	53
Crystalline Silicon Manufacturing.....	54
Wafer Dicing.....	55
Wafer Doping.....	56
Laser-Fired and Grooved Contacts.....	57
Wrap-Through Technologies	57
Thin-Film Manufacturing	58
Laser Scribing.....	58
Laser Edge Isolation/Deletion	60
Laser Crystallization	60
Laser Nanolithography	61
Laser-LIGA (Lithography, Electroplating, and Molding).....	63
Characterization Techniques	63
Photoluminescence	63
Shunt Detection	64
Quantum Efficiency Measurements	65
Solar Simulation	66
Conclusion	66
Acknowledgments	67
References.....	67

Introduction

In this chapter, we will discuss the impact that photonics have on photovoltaic (PV) manufacturing. The broad field of photonics is now commonly thought to encompass classical optics (Hecht, 2001), nanophotonics (Joannopoulos et al., 2007), and metamaterials (Cai and Shalaev, 2009). Over the last few decades, photonic technology has become an increasingly integral part of PV manufacturing, both in the crystalline silicon and thin-film arenas.

PV manufacturing has attracted increasing interest recently, thanks in part to its tremendous growth over the past decade. Innovative German feed-in tariffs have greatly facilitated this market growth, from 2.2 GW globally (373 MW EU) in 2002 to an estimated 37–38 GW installed globally in 2013. The last few years have also marked the arrival of low-cost manufacturing from China, with multicrystalline silicon average selling prices dropping from \$3.55/Wp in 2006 to \$0.66/Wp in 2013. The impact has been to make PVs competitive in price per kilowatt-hour with a wide variety of incumbent technologies in certain markets—an important concept known as *grid parity*.

Here, we will discuss the contributions of photonic technologies toward these dazzling achievements, while also identifying some key areas for future growth. For example, while most photonic tools employed in PV manufacturing at present are derived from classical optics, newer energy conversion technologies being developed in nanophotonic and metamaterial platforms may also become an integral part of PV manufacturing going forward.

This chapter will proceed along the following structure. First, we will discuss photonic technologies employed in crystalline silicon manufacturing, which include wafer dicing for dividing raw ingots into substrates for further processing; doping of the resultant wafers to suppress recombination; laser-fired and grooved contacts, which allow the creation of a back surface field that suppresses surface recombination and improves efficiency; and wrap-through technologies. The discussion will then continue onto thin-film manufacturing, including laser scribing and laser edge isolation and deletion. Finally, characterization techniques needed for postmanufacturing quality assurance are discussed. These include photoluminescence for material identification, electroluminescence for shunt detection, quantum efficiency (QE) measurements, and solar simulation.

Crystalline Silicon Manufacturing

Ever since the first silicon-based PV cell was demonstrated by Bell Labs in 1954, synergy with the semiconductor industry has led crystalline silicon-based PV to play a dominant role over the last 59 years. The role of photonics in crystalline silicon, however, is somewhat more recent, in that it is mainly driven by laser-based technologies. The laser was invented in 1960 by Theodore Maiman, drawing on theoretical and experimental work performed by Schawlow and Townes. Since then, the key metrics for laser performance, including operating wavelength, optical power, coherence, and affordability, have all improved by orders of magnitude compared to the earliest experiments. This technology has now become ubiquitous enough that it can now replace incumbent manufacturing technologies while also

adding new efficiency-boosting features to crystalline silicon cells that were not previously possible to include in manufacturing without photonics.

Wafer Dicing

All crystalline silicon solar cells are built on the foundation of the silicon wafer. A properly prepared silicon wafer offers the following combination of features, necessary for high-performance PV cells: ultrahigh purity, high carrier mobility, and low nonradiative recombination. It is also helpful but not absolutely mandatory to have a monotonically varying band structure with a back surface field to enhance carrier extraction near the terminals.

Underlying all these features is the raw material requirement of ultrahigh-purity crystalline silicon. Generally, electronics-grade polysilicon with eight nines of purity is melted and then extracted as a large mass through the float-zone or Czochralski process (Streetman and Banerjee, 2000). Afterwards the resulting silicon boule must then be diced into pieces with a thickness that ensures sufficient optical absorption without excessive carrier recombination. In the world record-setting 25.0% efficient crystalline silicon cell, known as the PERL cell from Martin Green's group at the University of New South Wales, a thickness of 450 μm is employed.

Typically, wafers are created from the boule via mechanical sawing. In this process, a thin diamond-tipper blade saw or wire saw is used to physically separate pieces with the target thickness from the boule, one at a time, in rapid succession (Streetman and Banerjee, 2000). Wafers emerging from this process require further postprocessing to be rendered flat enough for photolithographic processing and chamfering along the edges to reduce the probability of chipping during processing. Furthermore, in many cases, a chemical-mechanical polish with a slurry of fine particles (e.g., silica or ceria) is employed to achieve a flat surface on at least one side. In many cases, this is followed by etching with an alkaline (high pH) solution, in order to roughen the surface to assist with light trapping. However, this process also has certain drawbacks. One is that approximately 50% of the material is wasted as saw dust, which is technically known as kerf loss. The second is that it requires multiple mechanical and chemical processing steps, which take time and even require rare earths (such as cerium) for some versions of the process.

A new alternative to the die saw method is laser-based dicing. In this approach, the energy of the laser beam replaces the mechanical sawing action. This can be thought of metaphorically as an *optical knife*. There are two basic strategies for laser-based dicing: conventional and stealth dicing. In conventional laser-based dicing, one utilizes a wavelength that is strongly absorbed by the target, which locally heats it enough to cause vaporization and removal from the target area, which then clears the way for further cutting. Since silicon has an indirect bandgap wavelength of 1107 nm, such a laser would generally be in the visible or near-infrared.

In stealth laser-based dicing, one instead utilizes a wavelength that is typically not absorbed directly by the substrate but requires a nonlinear absorption process (generally two-photon absorption). In this case, multiple beams from different directions can be focused to create localized point-like or linear high-intensity regions inside the material. The nonlinear effect then ensures that the cutting action will occur only at the high-intensity regions.

Wafer Doping

In order to introduce the correct band structure for crystalline silicon wafers, necessary for high performance, dopant diffusion is required. Most commonly, the silicon wafers are grown as p-type and then doped with an n-type front region through phosphorous gas (POCl) diffusion. In such cases, it is well known that the diffusing particles will observe Brownian motion. This process is quantified by Fick's law and allows the doping profile to be tuned by adjusting both the doping time and temperature. The latter is generally a particularly sensitive parameter, since such processes generally follow the Arrhenius equation, with an exponential dependence on temperature. At the same time, most substrates have a limited *thermal budget*, that is, a maximum time-temperature product that they can bear during processing. As a result, most doping is performed using a rapid-thermal annealing machine (Streetman and Banerjee, 2000).

An alternative method that offers greater control over doping profile is known as ion implantation. In this process, dopants are accelerated by a high voltage and separated by a magnetic field en route to the target. Adjusting the type, energy, and angle of the ions can fine-tune the implanted doping profile. However, the cost of this method is very high, due to the need for a beamline and relatively low throughput. As such, it is not generally deployed in semiconductor manufacturing.

In laser doping, one combines the best of both worlds: the relatively modest costs of dopant diffusion with the more precise control and lack of thermal stress associated with ion implantation. In this approach, a doping precursor is first deposited on the target, to serve as an ion source. Then the process is engaged by scanning the entire surface where doping is required with a pulsed laser beam. It is currently believed that the laser pulse will rapidly and locally heat the doping precursor as well as the top surface of the silicon. Some of the doping precursors will then rapidly diffuse into the target, while the rest evaporates. At the end, one is left with a doped silicon wafer and an unchanged substrate.

The most popular tool for laser-based doping is a green Nd:YAG laser, operating at 530 nm. It combines a high repetition rate of 10 kHz and a small spot diameter of 0.1 mm with sufficient beam fluence. Alternatives include ruby lasers (694 nm, 5 Hz repetition, and 9 mm beam spot) as well as excimer lasers (ArF, 193 nm, 10 Hz repetition, 20 mm² spot).

Laser-Fired and Grooved Contacts

Discussion will then proceed to laser-fired and grooved contacts and the results of the induced back surface field on cell performance.

Laser-fired contacts offer a unique approach to improving the performance of solar cells, based on redesigning the design of the back contacts. The common, straightforward method of placing a eutectic metal backing directly behind a silicon wafer has several disadvantages. First, the reflection is generally suboptimal, because the group velocity of light in silicon is well below that of air. Second, the work function of the metal can create a Schottky barrier, which impedes the smooth flow of current through the structure to the electrical contacts. Third, the surface recombination velocity associated with the silicon-metal interface can be relatively high, which degrades the PV cell power conversion efficiency (particularly the open-circuit voltage). With laser-fired contacts, one first creates a low-refractive-index layer behind the silicon wafer, either through native oxide growth or through deposition. Then holes are drilled in the low-index material with laser cutting, for example, with an ultraviolet wavelength excimer laser. Then the eutectic metal is then used to fill in the holes and coat the back. This strategy has several advantages, which include increasing the reflectivity of the base metal via the higher group velocity in the low-index material, decreasing or eliminating any Schottky barriers previously present, and creating a back surface field to facilitate the flow of electrons and decrease surface recombination. The combined effect is a quantifiable improvement in the short-circuit current.

Laser-grooved contacts are of interest for similar reasons. In this approach, invented by Martin Green and Stuart Wenham of the University of New South Wales, one uses lasers to groove the front of the wafer. This provides an opportunity for secondary dopant diffusion near the surface, followed by electroplating. Several advantages can be achieved from this approach, including improved collection of long-wavelength photons; decreased shadowing, due to the narrower width of the busbars; and higher current-carrying capacity/lower series resistance, thanks to the greater cross-sectional area of the contacts.

Wrap-Through Technologies

Wrap-through technologies (metal wrap-through [MWT] and emitter wrap-through [EWT]) will then be shown to offer significant advantages in terms of reduced shadowing and improved module-level integration.

The MWT cell design concept was devised by van Kerschaver and collaborators (1998). MWT functions by shifting half of the front contacts of a solar cell toward the back, in order to reduce shadowing losses by a proportional fraction. In this process, holes are periodically drilled in the PV active material using a high-throughput laser. Next, a metal paste (known as a eutectic) is filled in from behind, in order to connect the front and back

regions of the cell. The net effect is to increase power production more than the additional cost of this processing step. While the idea has been well known for some time, the first prototype production came online in 2007 at Fraunhofer ISE in Germany. The multicrystalline silicon cells produced offered a 16% average efficiency, about a 0.5% absolute improvement over the standard design without MWT (Clement et al., 2010).

EWT was proposed by James M. Gee and collaborators (1993). It consists of interdigitated p- and n-type metallic back contact grids, with highly conductive vias drilled to the n+-doped front layers. This, in many ways, resembles laser backfired contacts but with deeper drilling for the n-type grid. This design offers several features that contribute to high performance, including low shadowing and low resistivity due to the geometry of the contacting approach, natural alignment between the drilled vias and metallized n-type grid, and separate emitter and contact diffusion steps for maximum fabrication control (Gee et al., 1993). For adequate industrial throughput, it has been estimated that to achieve a via spacing of 1 mm in each direction, each individual via must be drilled in less than 6 ms.

Thin-Film Manufacturing

Thin-film photovoltaics (PVs) represent a paradigm shift in PV manufacturing. In the last decade, quality has greatly improved in most market segments, including cadmium telluride (CdTe), as promising new technologies demonstrate enhanced commercial viability, including gallium arsenide (GaAs), copper indium gallium diselenide (CIGS), and organic heterojunctions.

In this part, a different set of laser-based techniques for thin-film manufacturing (micromorph, CdTe, CIGS, and CZTS) will be discussed. The primary focus will be on cell definition and module integration approaches.

Laser Scribing

In particular, laser scribing will be shown to play a critical role in enabling monolithic integration over very large sheets of glass, necessary for economic competitiveness.

For monolithic integration of PV modules, it is important to have an approach to connect the front and back of a large array of cells. This allows for maximum power output with much lower currents (for greater efficiency and safety), plus significantly higher voltages (since the maximum power point voltage of a single silicon cell is approximately 0.6 V, whereas home outlets have a 110 V rms output). This goal can be achieved by scribing three cuts at each line of interconnection. The first cut is an isolation step

performed before PV material deposition. It divides the front transparent conductive oxide (TCO) into electrically disconnected stripes. After the PV material is deposited, a second cut is performed through it. This creates a via from the back of the cell to the front TCO. Subsequently, a metal backing is conformally deposited all along the back surface. Finally, a third cut is performed in the metal backing, closely aligned with the first two cuts in order to force electricity to flow through the PV active material. A slight drawback to this method is small *dead* regions caused by the surface area associated with the scribe features, which limits the density of scribe lines to approximately 1 cm spacing.

There are three serious candidates for large-scale production of scribe lines: photolithography, mechanical scribing, and laser scribing. In the first method, photolithography, a photoresist is deposited and then spun to uniformity. Then an optical mask and light source is used to create the desired pattern in the photoresist. A selective etching process (such as a chemical wet etch or reactive ion etch) is then employed to remove the underlying material. Finally, the remaining photoresist is removed. However, this approach is fairly time-consuming, complex, low throughput, and expensive—as a result, it is not widely used. The second method, mechanical scribing, is much simpler, in that it uses a sharp blade embedded on a stylus to physically separate the deposited layers. In principle, this approach is highly appealing in terms of simplicity and cost. While this approach works well for soft materials, including metallic pastes and certain active PV materials (particularly CdTe), it is not as suitable for etching TCOs with high haze factors, due to their mechanical roughness, as required for the first scribing step. In those cases, the channels formed are jagged and not accurate enough to meet the specifications of high-end manufacturing. As a result, a third strategy, based on laser patterning, has come to be much more widely used for one or more of the scribing steps. In this strategy, a high-intensity pulsed laser with picosecond durations is employed for cold ablation of the targeted surface—that is, the laser is delivered so quickly that the thin film does not suffer any heat damage. The net result is to create clean, precisely defined channels on the surface of each layer at high speed (on orders of meters per second) and to a depth controlled to an accuracy of 20 nm (Shin et al., 2011).

In terms of the lasers suitable for scribing, it has been found that a wide variety can be used, including Nd:YAG at both 1064 and 532 nm (frequency-doubled), copper vapor at both 510.6 and 578.2 nm, and excimer lasers using xenon chloride (308 nm) and krypton fluoride (248 nm) (Compaan et al., 2002). Generally, scribing can be achieved with pulse energies approximately ten times the threshold for surface damage at the wavelength used. The damage threshold for opaque materials is typically 0.5 J/cm^2 over a broad range of wavelengths. However, the thresholds are significantly higher for optically transparent materials such as TCOs, due to a lack of absorption, unless

one reaches ultraviolet wavelengths with excimer lasers. For a scribe width of 40 μm , 200 mJ delivered energy is required for each meter of scribing. Since Nd:YAG lasers typically deliver 1 mJ, a rapid succession of pulses is required to scribe appreciable distances on the solar cell. At a repetition rate of 1 kHz, each line will take 0.2 s to scribe. Since excimer lasers generally deliver much more pulse energy (e.g., 400 mJ) than Nd:YAG lasers, it generally suffices to print even the largest form factor modules in a single pulse. At a repetition rate of 50 Hz, each line will take 0.02 s to scribe.

Laser Edge Isolation/Deletion

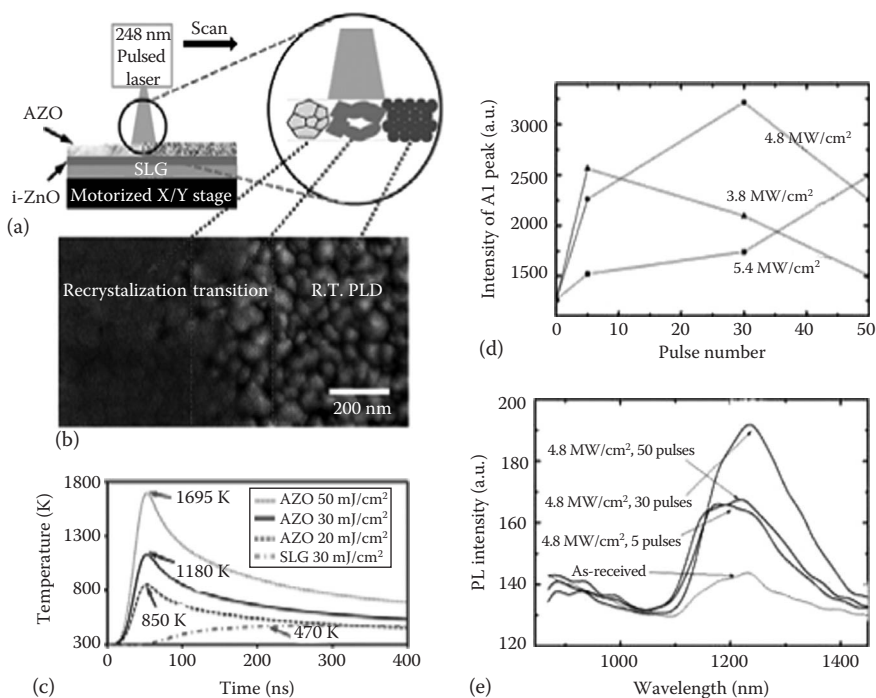
Laser edge isolation/deletion has been shown to be helpful in maximizing performance and also have some cross industry relevance in crystalline silicon manufacturing. Emerging techniques such as laser-induced *in situ* crystallization, interference lithography, and laser-LIGA are also discussed.

Laser edge isolation can be achieved by using a laser scribe (from Section 3.3.1) to define a groove around the outermost edge of the solar cell. It is important for the groove to extend deep enough through the n+ front-doped region into the bulk p-type region, in order to minimize shunting.

Laser Crystallization

Laser-induced *in situ* crystallization is a technique under recent development, in which a high-power pulsed laser is utilized to increase the grain size and decrease the defect density of a deposited thin film of PV material (Cheng et al., 2012 and Cheng and Zhang, 2013). The current thin-film PV has the following problems: (1) Low formation temperature leads to recombination of excess minority carriers in the active absorber, and (2) low reaction kinetics of near vacuum vapor processes limits maximum achievable throughputs in current thin-film PV manufacturing. Here, we will develop direct laser crystallization (DLC) of nanoparticle inks, a high-speed crystallization technique in which nanoparticles are rapidly heated and crystallized at ambient conditions. The novelties are as follows: (1) higher performance due to much lower defects, (2) high speed and scalability, (3) lower cost—due to the much better energy and materials usage, nanoparticles have much higher sinterability than bulk materials—and (4) selective heating, leading to scalable process on various substrates and different layers without affecting other layers.

Targeted materials under current investigation include aluminum-doped zinc oxide (AZO) and CIGS. Recent studies of laser crystallization in AZO have shown that the DLC process can increase the mobility significantly, thanks to a reduction in defect density and strain (Zhang and Cheng, 2011, 2012). The schematic of the process, simulation, and experimental results are shown in [Figure 3.1](#).

**FIGURE 3.1**

DLC of AZO nanoparticles: (a) schematic of DLC; (b) crystalline structures after DLC; (c) temperature profile at various layers; (d) crystallinity by Raman spectrum; and (e) photoluminescence. (From Zhang, M.Y. and Cheng, G.J., *Appl. Phys. Lett.*, 99, 051904, 2011; 2012.)

Laser Nanolithography

Fabricating high-performance 2D and 3D nanophotonic structures requires advanced lithography tools. While steppers are an industry standard, they are generally high in cost and suited primarily for large-scale manufacturing of 2D structures. Other lithography tools, such as laser writers and e-beam lithography, can be much lower in cost but also are impeded by throughput that is many orders of magnitude lower as well.

As an alternative, we are building the high-accuracy and high-throughput laser interference lithography approach depicted in Figure 3.2c. The principle behind this method is depicted in Figure 3.2a: two coherent laser beams of wavelength λ , when intersecting at a particular angle θ , will form a standing wave with a periodicity $\lambda/(2 \sin \theta)$. This standing wave can be recorded in a layer of photosensitive material, known as the photoresist. Upon immersion in a special chemical, the so-called developer, the areas of photoresist that experienced large optical intensities will be washed away, while areas that did not will remain unaffected. This will result in a grating pattern

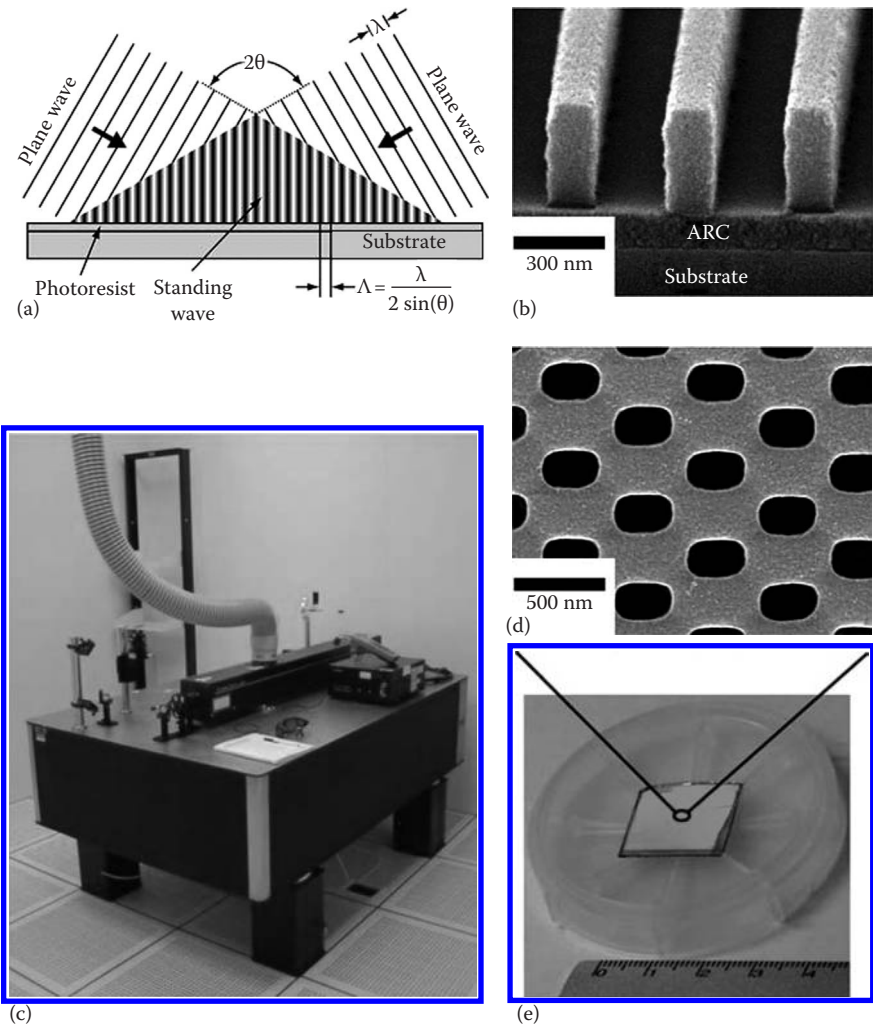


FIGURE 3.2 Interference lithography setup for 3D-integrated nanophotonic fabrication: (a) The basic concept is to create a standing wave that will be recorded in a photosensitive film (i.e., the photoresist). (b) SEM of a grating pattern formed by developing away exposed resist. (c) Snapshot of an interference lithography system at Purdue’s Birck Nanotechnology Center. (d) A 2D grid pattern formed by interference lithography after two consecutive exposures. (e) Snapshot illustrating the extensive, uniform coverage of this technique over 4 cm².

(Figure 3.2b). If two consecutive exposures are conducted before the photoresist is developed, a grid pattern, such as the one in Figure 3.2d, will appear. This pattern will be the starting point for our angled etching. An exposure setup with a 248 nm wavelength KrF excimer laser inside a class-10 clean room, run jointly by Prof. Bermel and Prof. Qi, is depicted in Figure 3.2e. The iridescent green color evident in the photograph demonstrates the presence of uniform wavelength-scale 2D periodicity.

Laser-LIGA (Lithography, Electroplating, and Molding)

Laser-LIGA is a technique for forming high-aspect-ratio nanostructures, such as encapsulant materials for protecting PV modules from environmental degradation. It involves the following three steps: lithography, electroforming, and molding (Kathuria, 2004). In the original version of LIGA, the lithography step was performed using synchrotron x-rays for high spatial resolution at the nanoscale and utilized a specially designed x-ray mask, using high-atomic-weight scattering materials, and an x-ray-sensitive resist, such as PMMA. In laser-LIGA, an analogous process is pursued, in which lasers serve an analogous role as x-rays. However, the laser-based process is substantially more widely accessible and much lower cost, due to the relative ubiquity of laser sources such as KrF excimer lasers, as well as the relatively commonality of masks and resists (e.g., SU-8) that are suitable for the UV wavelengths produced by such sources. In either case, the next step consists of electroplating the lithographically formed structure with a metal of interest—common choices include nickel, copper, and gold. The resulting metallized structures can then be used as a mold for mass-producing inverted structures made from common injection molding materials, such as epoxy or polyethylene.

Characterization Techniques

In this section, new and emerging techniques for PV cell and module characterization are discussed: photoluminescence for material identification, infrared shunt detection, QE measurements, and broadband solar simulation.

Photoluminescence

Photoluminescence (PL) is a useful procedure for rapid in-line materials characterization, particularly for relatively novel PV materials. Key information that can be extracted from PL includes electronic bandgap, minority carrier lifetime, and quasi-Fermi level splitting. In this approach, one injects current into the material of interest and measures the energy spectrum of

the resulting photons emitted. The rationale for this approach is that in a reasonably high-quality semiconductor material, the radiative lifetime will at least be within a few orders of magnitude of the nonradiative lifetime. This means that if both electrons and holes are present in the conduction and valence bands, respectively, there will be a nonnegligible probability of radiative recombination. The current injection serves to increase this probability substantially, improving the signal-to-noise and detection rate. The resulting emission spectrum will begin very nearly at the bandgap (neglecting excitons) but extend at least one or two thermal voltages above that energy as well. The line shape of the resulting spectrum will reflect the joint density of states of the system, which can be used to work backward to determine the relative flatness of the conduction and valence bands. If periodic photonic excitations are applied and the resulting re-emitted photons are resolved carefully in time, this can give rise to the related time-resolved PL (TRPL) technique, which directly measures minority carrier lifetime under both high-injection and low-injection conditions.

On a related note, electroluminescence techniques can be used to measure the external fluorescence efficiency (also known as the external radiation efficiency [ERE]). This quantity is significant because it sets an upper bound to the device performance (specifically, the open-circuit voltage).

Shunt Detection

Shunts in PV cells allow current to bypass its desired path through an extra electrical connection appearing through errors in the PV manufacturing process. Shunts can cause substantial degradation in performance at the cell level. At the module level, the effects can be even worse, since standard series interconnections mean that individual cells with significant shunting tend to degrade the performance of their neighbors as well.

In order to address this issue, one can employ infrared photography in order to both detect and repair these shunts. Effectively, the cells are contacted and reverse biased, in order to force current through the cell. They are then imaged with an appropriate infrared camera to detect localized heating. For operation near room temperature, sensitivity out to 9 μm , near the peak of the thermal emission spectrum, is ideal, although sensitivity to 5 μm may be sufficient. This wavelength sensitivity can be achieved through several routes, including platinum silicide and mercury CdTe-based detectors. In many cases, it is important to record the images immediately after the current is injected (within a few seconds), or the heating can spread throughout the cell, obscuring the source of the problem.

In order to address the problems detected through this technique, several strategies are possible. Especially with thin films, one can potentially use a point-like laser scribe to etch away or remove the shunt region. An alternative is to electrically isolate it, although the exact procedure depends on the level at which the shunt is detected. For shunts detected at the cell level, one

can add another electrical contact to reduce the impact of the shunt or at the module level by adding a bypass diode to connect the neighbors of the shunted cell.

Quantum Efficiency Measurements

A pair of important measurements of the spectral response of a solar cell can be grouped together as QE measurements. The first QE measurement is internal quantum efficiency (IQE), which captures the probability that an absorbed photon is collected as a corresponding unit of electrical current. The second QE measurement, external quantum efficiency (EQE), is the probability that an incident photon from outside will be converted into a corresponding unit of current. It is also equal to the product of the IQE and the absorption probability $A(\lambda)$. Both QE measurements can range from 0% to 100%, but EQE will always be bounded from above by the IQE.

Measuring QE accurately is a nontrivial task. While several strategies have been implemented experimentally, the basic premise of most techniques is as follows. Generally, since IQE cannot be measured directly, one generally measures EQE, transmission, and reflection at each wavelength separately. Then the IQE is obtained as the quotient of the EQE and the inferred absorption. Finding the EQE requires a setup with a few key elements: a calibrated source lamp with significant emission over the range of interest, a monochromator allowing one to select a single wavelength at a time, a receiver calibrated over that same range, and the ability to contact and measure the targeted solar cell. It is also highly recommended to have a computer-based controller to automate this measurement procedure over the full spectrum of interest. Assuming the calibration for both source and receiver is accurate, the electrical current measured can be divided by the current from the reference system and multiplied by the reference EQE, in order to find the EQE for the sample of interest.

Detecting absorption as a means to subsequently determine IQE can take on different levels of complexity. For flat structures, it is generally sufficient to measure specular reflection and transmission only, which for a point-like source can be detected at specific locations easily predicted by geometric optics. Furthermore, most solar cells have negligible transmission due to a metallic back contact and can be assumed to vanish. For textured structures, however, diffuse reflection becomes a key component of loss. For greatest accuracy, one must then integrate the reflection over all angles to obtain all reflected rays. This function is generally performed by an integrating sphere, in which a source and detector are placed in specific small locations within a large sphere and the rest of the interior is coated with a bright white diffuse scatterer. Given proper calibration, this method can accurately determine the full reflection (combining both diffuse and specular components). In any case, once all reflection components are accounted for, the absorption is taken to be unity less the total reflection. The EQE is then divided by the absorption to obtain the IQE measurement.

Solar Simulation

While the EQE measured in the previous section can be used to predict the short-circuit current with reasonably good accuracy, the overall power conversion efficiency often cannot be, due to uncertainties in the open-circuit voltage and fill factor. This gives rise to the need for solar simulation testing. In this procedure, one creates a standardized spectrum of light in which to operate a PV cell and then measures the output current as a function of the bias voltage applied to the cell (known as the light I-V curve). The current at zero applied voltage is the short-circuit current I_{sc} , and the voltage when the current vanishes is the open-circuit voltage V_{oc} . Since output power is the product of the current and voltage, the maximum power output can also be easily obtained from this test. The quotient of the maximum power output with respect to the product of I_{sc} and V_{oc} is the fill factor.

Clearly, the standard spectrum of light must be well defined in terms of relative wavelength intensities, as well as overall intensity, for this procedure to make sense. Great variability with location, weather, time of year, and time of day means that careful studies are needed to establish standards consistent with the real operating conditions of solar cells. ASTM-G173 established the two most well-known and accepted standards: AM0 (air mass zero) for outer space, and AM1.5 (air mass one and a half) for terrestrial applications. The corresponding powers for each case are 1.366 and 1 kW/m². The AM1.5 spectrum has less light, particularly in the blue portion of the spectrum, due to Rayleigh scattering, as well as some atmospheric absorption in certain wavelength bands (e.g., from water vapor). In order to reproduce the AM1.5 spectrum in a laboratory, one generally needs a broadband high-thermal-temperature source (to mimic the sun), such as a xenon arc lamp. The output light must then be spectrally filtered with a series of filters to closely match the target spectrum.

Conclusion

In conclusion, we demonstrated a broad range of applications for photonic and laser technologies toward PV manufacturing. For crystalline silicon manufacturing, it was shown that laser-based wafer dicing offers improved materials usage, laser-based doping provides an alternative to high-temperature diffusion suitable for reducing thermal budgets, laser-fired and grooved contacts suppress surface recombination, and EWT and MWT technologies offer lowered shadowing and series resistance. It was also shown that thin-film manufacturing can benefit from laser scribing for series interconnection, laser edge isolation and deletion for reduced surface recombination, and DLC for improved minority carrier lifetimes and mobilities, as well as

two related lithography techniques, interference lithography and laser-LIGA. Finally, four optical characterization techniques for quality assurance in PV manufacturing were discussed: photoluminescence for material identification, infrared shunt detection, QE measurements, and solar simulation.

Acknowledgments

The authors thank Ashraf Alam, Ryyan Khan, Mark Lundstrom, Minghao Qi, and Ali Shakouri for useful discussions. Support was provided by the Department of Energy, under DOE Cooperative Agreement No. DE-EE0004946 ("PVMi Bay Area PV Consortium"), as well as the Semiconductor Research Corporation, under Research Task No. 2110.006 ("Network for Photovoltaic Technologies.")

References

- Bartlome, R., Strahm, B., Sinquin, Y., Feltrin, A., and C. Ballif, Laser applications in thin-film photovoltaics, *Appl. Phys. B* 100, 427–436 (2010).
- Cai, W.-S. and V. Shalaev, Optical Metamaterials: *Fundamentals and Applications*. Springer, New York, (2009).
- Cheng, G.J., M.Y. Yang, and Y. Zhang, High speed laser crystallization of nanoparticle inks for thin film solar cells, U.S. Patent application number US2012-0021559.
- Cheng, G.J. and M.Y. Zhang, Laser crystallization of thin film on various substrates, U.S. Patent application number US 2013-0075377.
- Clement, F. M. Menkoe, D. Erath, T. Kubera, R. Hoenig, W. Kwapil, W. Wolke, D. Biro, R. Preu, High throughput via-metallization technique for multi-crystalline metal wrap through (MWT) silicon solar cells exceeding 16% efficiency, *Sol. Energy Mater. Sol. Cells* 94, 51–56 (2010).
- Compaan, A.D., I. Matulionis, and S. Nakade, Optimization of laser scribing for thin-film PV modules, Final Technical Progress Report, NREL/SR-520-24842, University of Toledo, Toledo, OH (available from NTIS, 1998).
- Gee, J.M., W.K. Schubert, and P.A. Basore, Emitter wrap-through solar cell, *23rd IEEE Photovoltaic Specialists Conference*, Louisville, KY, pp. 265–270 (1993).
- Hecht, E., *Optics*, 4th edn. (Addison-Wesley, Reading, MA, 2001).
- Hermann, J.M. Benfarah, S. Bruneau, E. Axente, G. Coustillier, T. Itina, J.-F. Guillemoles, and P. Alloncle, Comparative investigation of solar cell thin film processing using nanosecond and femtosecond lasers, *J. Phys. D: Appl. Phys.* 39, 453–460 (2006).
- Huber, H.P., F. Herrnberger, S. Kery, and S. Zoppel, Selective structuring of thin-film solar cells by ultrafast laser ablation, *SPIE* 6881, Commercial and Biomedical Applications of Ultrafast Lasers VIII, 17 (2008).

- Joannopoulos, J.D., J.N. Winn, R.B. Meade, and S.G. Johnson, *Photonic Crystals: Molding the Flow of Light* (Princeton University Press, Princeton, NJ, 2007).
- Kathuria, Y.P., L3: Laser, LIGA, and lithography in microstructuring, *J. Indian Inst. Sci.* 84, 77–87 (2004).
- Shin, Y.C., G.J. Cheng, W. Hu, M.Y. Zhang, and S. Lee, High Precision Scribing of Thin Film Solar Cells by a Picosecond Laser, *Proceedings of NSF Engineering Research and Innovation Conference*, Atlanta, GA (2011).
- Streetman, B.G. and S. Banerjee, *Solid State Electronic Devices* (Prentice Hall, Englewood Cliffs, NJ, 2000).
- van Kerschaver, E., R. Einhaus, J. Szlufcik, I. Nijs, and R. Mertens, A. A novel silicon solar cell structure with both external polarity contacts on the back surface, *Proceedings of the Second World Conference on Photovoltaic Energy Conversion*, Vienna, Austria, Vol. 2, pp. 1479–1482 (1998).
- van Kerschaver, E., S. DeWolf, and J. Szlufcik, Toward back contact silicon solar cells with screen-printed metallization, *28th IEEE Photovoltaic Specialists Conference*, Anchorage, AK, pp. 209–212 (2000).
- Wiedeman, S., R.G. Wendt, and J.S. Britt, Module interconnects on flexible substrates *AIP Conference Proceedings*, Vol. 462, pp. 17–22 (1999).
- Wolden, C.A., J. Kurtin, J.B. Baxter, I. Repins, S.E. Shaheen, J.T. Torvik, A.A. Rockett, V.M. Fthenakis, and E.S. Aydil. Photovoltaic manufacturing: Present status, future prospects, and research needs, *J. Vac. Sci. Technol. A* 29, 030801 (2011).
- Zhang, M.Y. and G.J. Cheng, Highly conductive and transparent alumina-doped ZnO films processed by direct pulsed laser recrystallization at room temperature, *Appl. Phys. Lett.* 99, 051904 (2011).
- Zhang, M.Y., Q. Nian, and G.J. Cheng, Room temperature deposition of alumina-doped zinc oxide (AZO) on flexible substrates by direct pulsed laser recrystallization, *Appl. Phys. Lett.* 100, 151902 (2012).